PHYSICAL REVIEW A VOLUME 40, NUMBER 7 OCTOBER 1, 1989

Moment method applied to gaseous electronics

J. H. Ingold
Advanced Technology Department, GE Lighting, General Electric Company, Cleveland, Ohio 44112
(Received 15 May 1989)

The five-moment method in gaseous electronics is based on a model velocity distribution function with position-dependent parameters, such as density (one moment), average velocity (three moments), and average energy (one moment). Temporal and spatial dependence of these parameters is determined by solution of velocity moments of the Boltzmann equation, which are coupled, partial differential equations in time and space. In this paper velocity moments of the Boltzmann equation, including moments of the collision integral for elastic and inelastic collisions, are given for two model distribution functions—shifted Maxwellian and shifted shell—and solved for the case of a planar Townsend discharge in helium, including nonequilibrium regions near electrodes. Based on a comparison between calculated and measured values of α/N versus E/N, it is concluded that five-moment theory based on a shifted Maxwellian distribution is superior to either the five-moment theory based on a shifted shell distribution, or the two-moment theory based on a monoenergetic beam distribution.

I. INTRODUCTION

In physical situations where average velocity and average energy of electrons do not change in time or space, electrons are said to be in equilibrium with the electric field. In these situations, the energy imparted to electrons by a steady, uniform electric field is exactly balanced by energy lost in elastic and inelastic collisions with heavy particles. The steady, uniform motion of electrons under these conditions is accurately described by transport and rate coefficients which by custom are parametrized by E/N, the ratio of electric field to gas density.

Theoretical analysis of nonequilibrium situations in gaseous electronics is considerably more complicated than that of equilibrium situations, because time and space derivatives in the Boltzmann equation for the electron-energy distribution function (EEDF) must be taken into account. Near those points where the electric field varies abruptly in time or space, or near electrodes and insulating walls, electrons generally are not in equilibrium with the electric field. Consequently, parametrization of transport and rate coefficients by E/N is not possible.

There are several analytical techniques available to the theoretician wishing to investigate nonequilibrium situations, including numerical simulation by Monte Carlo calculation, numerical solution of the Boltzmann equation, either directly or by the spherical-harmonic expansion technique, and solution of the Boltzmann equation by the moment method. For example, the Monte Carlo technique has been used to investigate electron swarm behavior in steady, nonuniform fields in nitrogen.[1] The authors conclude that the numerical task is a formidable one, and suggest that a hydrodynamic approach, i.e., a moment method, is more desirable. Examples of numerical solution of the Boltzmann equation include investigation of the effect of sudden changes in unsteady, uniform fields in the positive column,[2] and the effect of steady, nonuniform fields in the cathode fall.[3] The moment method has been used to investigate nonequilibrium effects in the cathode fall[4] and in the modulated positive column,[5] and the effect of ionization on transport coefficients.[6]

Of these three techniques, numerical solution of the moment equations is the least time consuming. However, the moment method is also the least accurate, because the EEDF is assumed, not calculated. Consequently, the rates of those processes which depend on detailed knowledge of the EEDF, such as inelastic collision rates, are inaccurately calculated. Nevertheless, mass, momentum, and energy are conserved, so that qualitative estimates are easily obtained with moment methods.

In this paper, velocity moments of the Boltzmann equation, including moments of the collision integral, are given for two model distribution functions: shifted Maxwellian and shifted shell. For illustrative purposes, calculated results for α/N versus E/N in a steady, uniform electric field in helium with infinite electrode separation are compared with measurement, where α is Townsend's first ionization coefficient. It is shown that calculated results for the shifted Maxwellian distribution agree more closely with measurement over a wider range of E/N than those for the shifted shell distribution. In addition, calculated results for α and average energy versus position in a steady, uniform field with finite electrode separation are compared with published Monte Carlo calculations. It is shown that calculated results for the shifted Maxwellian distribution agree more closely with Monte Carlo calculations, and that calculated results for both distributions agree more closely with Monte Carlo calculations than those based on the single beam model.[7]

II. BACKGROUND THEORY

The Boltzmann equation for electrons in an electric field $\mathbf{E}$ is

$$\frac{\partial f}{\partial t}+\mathbf{c}\cdot\nabla_r f-\frac{e}{m}\mathbf{E}\cdot\nabla_c f=Cf\ , \quad (1)$$

where $f=f(t,\mathbf{r},\mathbf{c})$ is the EEDF, e and m are the electron charge and mass, and C is the collision operator. In what follows, it is useful to make the definition

$$n\langle g(\mathbf{c})\rangle \equiv \int g(\mathbf{c})f\, d^3c\ , \quad (2)$$

where $g(\mathbf{c})$ is any function of $\mathbf{c}$. For example, average velocity $\mathbf{c}_0$ is defined by the equation

$$n\langle \mathbf{c}\rangle \equiv \int \mathbf{c}f\, d^3c \equiv n\mathbf{c}_0\ . \quad (3)$$

By convention, the distribution function is normalized so that $\int f\, d\mathbf{c}=n$, where n is the electron density and the integration extends over all values of velocity $\mathbf{c}$. Moment equations are derived by multiplying both sides of Eq. (1) by various powers of electron velocity $\mathbf{c}$ and integrating over velocity space.

The first moment equation is obtained by multiplying the Boltzmann equation by unity and integrating, giving the continuity equation. For the case where one positive ion and a new electron are created by the impact of an energetic electron on an atom, the continuity equation is

$$\frac{\partial n}{\partial t}+\nabla\cdot n\mathbf{c}_0=\nu_i n\ , \quad (4)$$

where ν_i is the average ionization frequency defined by the relation

$$\nu_i=N\langle Q_i(c)c\rangle\ , \quad (5)$$

in which $Q_i(c)$ is the cross section for ionization by electrons with energy of $\frac{1}{2}mc^2$. The term on the right-hand side of Eq. (4) is derived as follows. The form of the collision operator C is such that[8]

$$\int g(\mathbf{c})Cf\, d^3c=\int [g'(\mathbf{c})-g(\mathbf{c})]NQ_j(c)cf\, d^3c\ , \quad (6)$$

where Q_j is the cross section for collisions of type j, and the quantity $g'(\mathbf{c})-g(\mathbf{c})$ is the change in $g(\mathbf{c})$ due to collisions. In the simplified form expressed by Eq. (6), it has been assumed that $m/M \ll 1$, where M is the atomic mass of the gas. For example, in an ionization event, $g'=2$ and $g=1$, so that the right-hand side of Eq. (4) follows directly from Eqs. (5) and (6).

The second moment equation, in reality three equations for the three components of the average velocity, is obtained by multiplying the Boltzmann equation by $\mathbf{c}$ and integrating, giving the following momentum balance equation to first order in the ratio m/M:

$$\frac{\partial n\mathbf{c}_0}{\partial t}+\nabla\cdot n\langle \mathbf{cc}\rangle+\frac{e}{m}n\mathbf{E}=-\nu_m n\mathbf{c}_0 \quad (7)$$

where ν_m is the average momentum-transfer collision frequency defined by the relation

$$\nu_m\mathbf{c}_0=N\langle Q_m(c)c\mathbf{c}\rangle\ , \quad (8)$$

in which $Q_m(c)$ is the cross section for momentum transfer by electrons with an energy of $\frac{1}{2}mc^2$. Because Eq. (7) is a vector equation, there are three momentum equations in the most general case. However, in one-dimensional problems such as those discussed below, only one momentum equation is needed. Nevertheless, to be consistent with published literature, the moment method discussed in this paper is referred to as the five-moment method.

The third moment equation is obtained by multiplying the Boltzmann equation by $\frac{1}{2}mc^2$ and integrating, giving the following energy balance equation to first order in the ratio m/M:

$$\frac{\partial}{\partial t}n\langle \tfrac{1}{2}mc^2\rangle+\nabla\cdot n\langle \tfrac{1}{2}mc^2\mathbf{c}\rangle+en\mathbf{c}_0\cdot\mathbf{E}$$
$$=-2\frac{m}{M}\nu_\epsilon n\langle \tfrac{1}{2}mc^2\rangle-\nu_i neV_i-\nu_x neV_x\ , \quad (9)$$

where $V_{i,x}$ is the ionization, excitation potential of the gas, ν_ϵ is the average energy transfer collision frequency defined by the relation

$$\nu_\epsilon\langle \tfrac{1}{2}mc^2\rangle=N\langle Q_m(c)c(\tfrac{1}{2}mc^2)\rangle\ , \quad (10)$$

and ν_x is the average excitation frequency defined by the relation

$$\nu_x=N\langle Q_x(c)c\rangle\ , \quad (11)$$

in which $Q_x(c)$ is the cross section for excitation by electrons with energy of $\frac{1}{2}mc^2$.

The average values of the quantities defined above are evaluated below for two model distribution functions: shifted Maxwellian and shifted shell.

III. SHIFTED MAXWELLIAN

The shifted Maxwellian distribution (SMD) is

$$f(t,\mathbf{r},\mathbf{c})=n\left[\frac{m}{2\pi kT}\right]^{3/2}\exp\left[-\frac{m(\mathbf{c}-\mathbf{c}_0)^2}{2kT}\right]\ , \quad (12)$$

where k is Boltzmann's constant, and where density n, average velocity $\mathbf{c}_0$, and temperature T are functions of t and $\mathbf{r}$. This distribution has a Maxwellian form in the center-of-mass frame moving with average velocity $\mathbf{c}_0$. This distribution is normalized so that $\int f\, d\mathbf{c}=n$. Furthermore, it can be shown that $\int \mathbf{c}f\, d\mathbf{c}=\mathbf{c}_0$, and that $\int \frac{1}{2}mc^2 f\, d\mathbf{c}=\frac{3}{2}kT+\frac{1}{2}mc_0^2$. The temperature T is a measure of the width at half maximum of this distribution. The quantity $\frac{3}{2}kT$ is a measure of the average energy of random motion defined by the relation

$$\tfrac{3}{2}kT\equiv\langle \tfrac{1}{2}m(\mathbf{c}-\mathbf{c}_0)^2\rangle\ . \quad (13)$$

A. Evaluation of average quantities

For simplicity, it is assumed that the electric field is located along the *z axis*, and that all quantities have azimuthal symmetry about the *z axis*. Then density, average velocity, and average energy are functions of t, z only, and integrals of the form

$$\langle g(\mathbf{c})\rangle=\int_{-\infty}^{\infty}\int_{-\infty}^{\infty}\int_{-\infty}^{\infty}g(u,v,w)f(t,x,y,z,u,v,w)\times du\,dv\,dw\ ,$$

where x,y,z and u,v,w are Cartesian components of the vectors $\mathbf{r}$ and $\mathbf{c}$, can be simplified to the following:

$$\langle g(\mathbf{c})\rangle\equiv 2\pi\int_{0}^{\infty}\int_{-1}^{1}g(c,\mu)f(t,z,c,\mu)c^2dc\,d\mu\ , \tag{14}$$

where μ is the cosine of the angle between the z *axis* and the vector $\mathbf{c}$.

When the distribution has the form given by Eq. (12), then the z *components* of the various average quantities defined in Sec. II are calculated to be the following:

$$\langle w\rangle=w_0\ , \tag{15}$$

$$\langle ww\rangle=\frac{kT}{m}+w_0^2\ , \tag{16}$$

$$\langle \tfrac{1}{2}c^2w\rangle=w_0\left[\frac{5}{2}\frac{kT}{m}+\frac{1}{2}w_0^2\right]\ . \tag{17}$$

Elastic collision frequencies are given by the following expressions:

$$\frac{\nu_m}{N}=\left[\frac{kT}{2\pi m w_0^6}\right]^{1/2}\exp\left[-\frac{mw_0^2}{2kT}\right]\int_0^{\infty}\exp\left[-\frac{mc^2}{2kT}\right]\left[\left[\frac{mw_0c}{kT}\right]\cosh\left[\frac{mw_0c}{kT}\right]-\sinh\left[\frac{mw_0c}{kT}\right]\right]Q_m(c)c^2dc\ , \tag{18}$$

$$\frac{\nu_\epsilon}{N}=\frac{4}{3\sqrt{\pi}w_0}\left[\frac{m}{2kT}\right]^{3/2}\left[1+\frac{mw_0^2}{3kT}\right]^{-1}\exp\left[-\frac{mw_0^2}{2kT}\right]\int_0^{\infty}\exp\left[-\frac{mc^2}{2kT}\right]\sinh\left[\frac{mw_0c}{kT}\right]Q_m(c)c^4dc\ . \tag{19}$$

Equations similar to Eqs. (18) and (19) were derived by Morse.[9]

Inelastic collision frequencies are given by the following expression:

$$\frac{\nu_{i,x}}{N}=\frac{1}{w_0}\left[\frac{m}{2\pi kT}\right]^{1/2}\exp\left[-\frac{mw_0^2}{2kT}\right]\int_0^{\infty}\exp\left[-\frac{mc^2}{2kT}\right]\sinh\left[\frac{mw_0c}{kT}\right]Q_{i,x}(c)c^2dc\ . \tag{20}$$

B. Moment equations

The moment equations for SMD are found by substituting expressions derived above into the general moment equations derived in Sec. II. In order, the equations for particle balance, momentum balance, and energy balance for SMD are the following:

$$\frac{\partial n}{\partial t}+\frac{\partial(nw_0)}{\partial z}=\nu_i n\ , \tag{21}$$

$$\frac{\partial(nw_0)}{\partial t}+\frac{\partial}{\partial z}\left[n\left[\frac{kT}{m}+w_0^2\right]\right]-\frac{e}{m}nE=-\nu_m n w_0\ , \tag{22}$$

$$\frac{\partial}{\partial t}[n(\tfrac{3}{2}kT+\tfrac{1}{2}mw_0^2)]+\frac{\partial}{\partial z}[nw_0(\tfrac{5}{2}kT+\tfrac{1}{2}mw_0^2)]-enw_0E=-2\frac{m}{M}\nu_e n(\tfrac{3}{2}kT+\tfrac{1}{2}mw_0^2)-\nu_i neV_i-\nu_x neV_x\ , \tag{23}$$

where the collisions frequencies ν_j are given by Eqs. (18) to (20), and where it has been assumed that $\mathbf{E}=-E\mathbf{k}$ so that E is a positive quantity.

IV. SHIFTED SHELL

The shifted shell distribution (SSD) is[10]

$$f(t,\mathbf{r},\mathbf{c})=\frac{n}{2\pi s^3}\delta((\mathbf{c}-\mathbf{c}_0)^2-s^2)\ , \tag{24}$$

where electron density n, average velocity $\mathbf{c}_0$, and random speed s are functions of t and $\mathbf{r}$. This distribution has the form of a spherical shell in the center-of-mass frame moving with average velocity $\mathbf{c}_0$. The random speed s represents the radius of the shell, and the drift speed $\mathbf{c}_0$ represents the displacement of the center of the shell from the origin in velocity space. It is normalized so that $\int f\,d\mathbf{c}=n$. Furthermore, it can be shown that $\int \mathbf{c}f\,d\mathbf{c}=\mathbf{c}_0$, and that $\int \frac{1}{2}mc^2f\,d\mathbf{c}=\frac{1}{2}m(s^2+c_0^2)$. Therefore, by analogy with SMD, the random speed s is a measure of the "temperature" of the distribution. In other words,

$$\tfrac{3}{2}kT\equiv\langle \tfrac{1}{2}m(\mathbf{c}-\mathbf{c}_0)^2\rangle=\tfrac{1}{2}ms^2\ . \tag{25}$$

A. Evaluation of average quantities

As before, it is assumed that the electric field is located along the z axis, and that all quantities have azimuthal symmetry about the z axis. Then density, average velocity, and average energy are functions of t and z only, and integrals of the form

$$\langle g(\mathbf{c})\rangle\equiv\int_{-\infty}^{\infty}\int_{-\infty}^{\infty}\int_{-\infty}^{\infty}g(u,v,w)\times f(t,x,y,z,u,v,w)du\,dv\,dw\ ,$$

where x,y,z and u,v,w are Cartesian components of the vectors $\mathbf{r}$ and $\mathbf{c}$, and can be simplified to the following:

$$\langle g(\mathbf{c})\rangle\equiv 2\pi\int_0^{\infty}\int_{-\infty}^{\infty}g(p,w)f(t,z,p,w)p\,dp\,dw\ , \tag{26}$$

where $p^2=u^2+v^2$. It is helpful to express the velocity components p and w in the dimensionless form $\bar{p}=p/s$

and $\bar{w}=w/s$. Then Eq. (26) becomes

$$\langle g(\mathbf{c})\rangle=\int_0^\infty\int_{-\infty}^\infty g(\bar{p},\bar{w})\delta(\bar{p}^2+(\bar{w}-\bar{w}_0)^2-1)\bar{p}\,d\bar{p}\,d\bar{w}\ ,$$
$$=\tfrac{1}{2}\int_{\bar{w}_0-1}^{\bar{w}_0+1} g(\sqrt{1-(\bar{w}-\bar{w}_0)^2},\bar{w})d\bar{w}\ .$$

For example, suppose $g=w$; then $\langle g\rangle$ is calculated to be

$$\langle w\rangle=\frac{s}{2}\int_{\bar{w}_0-1}^{\bar{w}_0+1}\bar{w}\,d\bar{w}=w_0\ .$$

Likewise, for $g=ww$,

$$\langle ww\rangle=\frac{s^2}{2}\int_{\bar{w}_0-1}^{\bar{w}_0+1}\bar{w}^2 d\bar{w}=\tfrac{1}{3}s^2+w_0^2\ , \tag{27}$$

and for $g=\frac{1}{2}c^2w$,

$$\langle \tfrac{1}{2}c^2w\rangle=\frac{s^3}{2}\int_{\bar{w}_0-1}^{\bar{w}_0+1}(1-\bar{w}_0^2+2\bar{w}_0\bar{w})\bar{w}\,d\bar{w}$$
$$=w_0(\tfrac{5}{6}s^2+\tfrac{1}{2}w_0^2)\ . \tag{28}$$

Equations (27) and (28) are the same as Eqs. (16) and (17) when $\frac{3}{2}kT$ is identified with $\frac{1}{2}ms^2$.[10]

Following the same procedure, it can be shown that elastic collision frequencies are given by the following expressions:

$$\frac{\nu_m}{N}=\frac{s^3}{8w_0^3}\left[\frac{2e}{ms^2}\right]^2\times\int_{(m/2e)(s-w_0)^2}^{(m/2e)(s+w_0)^2}Q_i(\xi)\sqrt{2e\xi/m}\times\left[\xi-\frac{m}{2e}(s-w_0)^2\right]d\xi\ , \tag{29}$$

$$\frac{\nu_\epsilon}{N}=\frac{s^3}{4w_0(s^2+w_0^2)}\left[\frac{2e}{ms^2}\right]^2\times\int_{(m/2e)(s-w_0)^2}^{(m/2e)(s+w_0)^2}Q_i(\xi)\sqrt{2e\xi/m}\,\xi\,d\xi\ , \tag{30}$$

where the integration variable ξ is expressed in units of eV.

Likewise, inelastic collision frequencies have the form

$$\frac{\nu_{i,x}}{N}=\frac{s}{4w_0}\frac{2e}{ms^2}\int_{\xi_{\min}}^{(m/2e)(s+w_0)^2}Q_{i,x}(\xi)\sqrt{2e\xi/m}\,d\xi\ , \tag{31}$$

where the lower limit of integration is given by the relation

$$\xi_{\min}=\frac{m}{2e}(s-w_0)^2,\quad V_{i,x}<\frac{m}{2e}(s-w_0)^2$$
$$=V_{i,x},\quad V_{i,x}>\frac{m}{2e}(s-w_0)^2\ .$$

B. Moment equations

The moment equations for SSD are found by substituting the expressions derived above into the general moment equations derived in Sec. II. In order, the equations for particle balance, momentum balance, and energy balance for SSD are the following:

$$\frac{\partial n}{\partial t}+\frac{\partial(nw_0)}{\partial z}=\nu_i n\ , \tag{32}$$

$$\frac{\partial(nw_0)}{\partial t}+\frac{\partial}{\partial z}[n(\tfrac{1}{3}s^2+w_0^2)]-\frac{e}{m}nE=-\nu_m nw_0\ , \tag{33}$$

$$\frac{\partial}{\partial t}[n(\tfrac{1}{2}ms^2+\tfrac{1}{2}mw_0^2)]+\frac{\partial}{\partial z}[nw_0(\tfrac{5}{6}ms^2+\tfrac{1}{2}mw_0^2)]-enw_0E=-2\frac{m}{M}\nu_\epsilon n(\tfrac{1}{2}ms^2+\tfrac{1}{2}mw_0^2)-\nu_i neV_i-\nu_x neV_x\ , \tag{34}$$

where the collision frequencies ν_j are given by Eqs. (29) to (31).

V. DISCUSSION

In this section the following comparisons are discussed.

(1) Calculated results for α/N versus E/N in a steady, uniform electric field of finite extent in helium are compared with measurement.

(2) Calculated results for α and average energy versus position in a steady, uniform electric field of finite extent in helium are compared with published Monte Carlo calculations and Boltzmann calculations.

(3) Calculated results for average velocity and average energy versus E/N in a steady, uniform electric field of infinite extent in a model gas are compared with previous moment calculations.

The steady-state comparisons are based on simplified momentum and energy balance equations obtained by expanding the spatial derivatives on the left side of Eqs. (22) and (23) or Eqs. (33) and (34), and eliminating density n by means of Eq. (21) or Eq. (32), leaving two equations to be solved simultaneously for equilibrium values of drift energy $eU_d=\frac{1}{2}mw_0^2$ and random energy $eU_r=\frac{3}{2}kT$, or $eU_r=\frac{1}{2}ms^2$,

$$\left[1-\frac{U_r}{3U_d}\right]\frac{dU_d}{dz}+\frac{2}{3}\frac{dU_r}{dz}=E-\left[\frac{m}{2eU_d}\right]^{1/2}[2\nu_m U_d+\nu_i(2U_d+\tfrac{2}{3}U_r)]\ , \tag{35}$$

$$\frac{dU_d}{dz}+\frac{5}{3}\frac{dU_r}{dz}=E-\left[\frac{m}{2eU_d}\right]^{1/2}\left[2\frac{m}{M}\nu_\epsilon(U_d+U_r)+\nu_i(V_i+U_d+\tfrac{5}{3}U_r)+\nu_x V_x\right]\ . \tag{36}$$

For comparisons in helium, the collision frequencies ν_j appearing in Eqs. (35) and (36) are based on published theoretical values of momentum-transfer cross section[11] and of inelastic cross sections.[12] The momentum-transfer cross section is published in tabular form, and the inelastic cross sections are published in analytic form. A graph of the analytic expressions for helium inelastic cross sections used in the calculations is shown in Fig. 1. Curve A in Fig. 1 represents the sum of the cross sections for excitation to $n\,^1P$ levels with principal quantum numbers $n=2$ to 6, as given by Eq. (15) in the paper by Alkhazov,[12] except that it was found necessary to change the value of the parameter A' from 0.96 to 2.75 to recover the theoretical $n\,^1P$ cross sections shown in Figs. 3 and 4 of Alkhazov's paper.[12] Curve B in Fig. 1 represents the sum of the cross sections for excitation to $n=2$ to 6 levels with optically forbidden transitions, given by Eqs. (16a) to (16e) in Alkhazov's paper.[12] Curve C in Fig. 1 is the sum of curves A and B, and represents the total excitation cross section. For purposes of calculation, in other words, one lumped excited state with the excitation cross section given by curve C in Fig. 1 is assumed in the present work. The corresponding value of the excitation energy lost in one excitation event is assumed to be $eV_x=21$ eV, a value which is close to the mean of the six threshold energies of the three singlet and three triplet states included in curve C. Finally, curve D in Fig. 1 represents the ionization cross section given by Eq. (11) in Alkhazov's paper.[12] The corresponding value of the ionization energy lost in an ionization event is assumed to be $eV_i=24.5$ eV. While a discussion of the validity of the cross sections shown in Fig. 1 is beyond the scope of this work, it should be pointed out that Alkhazov[12] recommends values for the $3\,^1P$ and $4\,^1P$ cross sections which are about three-fourths of those measured,[13] while recommending a value for the $2\,^1P$ cross section which is about the same as that measured. This difference in the $3\,^1P$ and $4\,^1P$ cross sections translates to a difference in the total excitation cross section, represented by curve C in Fig. 1, of about 5% for a 100-eV electron.

A. Comparison with measurements of α/N

Electrons are said to be in equilibrium with the electric field when average velocity and average energy are invariant, a situation that is encountered in drift tube measurements of Townsend's first ionization coefficient α. Such experiments are simulated theoretically with the momentum and energy balance equations by setting derivatives of U_r and U_d equal to zero in Eqs. (35) and (36), giving two equations to be solved simultaneously for equilibrium values of drift energy $eU_d=\frac{1}{2}mw_0^2$ and random energy $eU_r=\frac{3}{2}kT$ or $\frac{1}{2}ms^2$,

$$\frac{E}{N}\left[\frac{2eU_d}{m}\right]^{1/2}=2\tilde{\nu}_m U_d+\tilde{\nu}_i(2U_d+\tfrac{2}{3}U_r)\ , \tag{37}$$

$$\frac{E}{N}\left[\frac{2eU_d}{m}\right]^{1/2}=2\frac{m}{M}\tilde{\nu}_\epsilon(U_r+U_d)+\tilde{\nu}_i(V_i+\tfrac{5}{3}U_r+U_d)+\tilde{\nu}_x V_x\ , \tag{38}$$

where $\tilde{\nu}_j\equiv\nu_j/N$, and the collision frequencies ν_j are given by Eqs. (18) to (20), or by Eqs. (29) to (31). By definition, Townsend's α is related to the ionization frequency ν_i by the equation

$$\frac{\alpha}{N}=\frac{\tilde{\nu}_i}{w_0}=\frac{\tilde{\nu}_i}{\sqrt{eU_d/m}}\ . \tag{39}$$

Results for α/N versus E/N for helium, calculated according to Eqs. (37) to (39) for both distributions, are compared with measurement[14] in Fig. 2. Note that good agreement between calculation and measurement is obtained for $E/N>3x10^{-16}$ V cm^2 for SMD. Results for the single-beam model (SBD) based on energy balance are also shown in Fig. 2. The single-beam result for α/N obtained from Eq. (38) and Eq. (39) by setting $U_r=0$, is

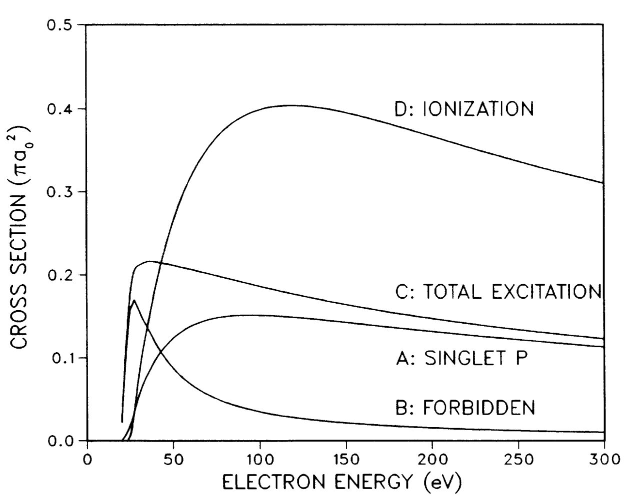

FIG. 1. Inelastic cross sections for helium used in the calculations. Analytic expressions for these curves obtained from Ref. 12.

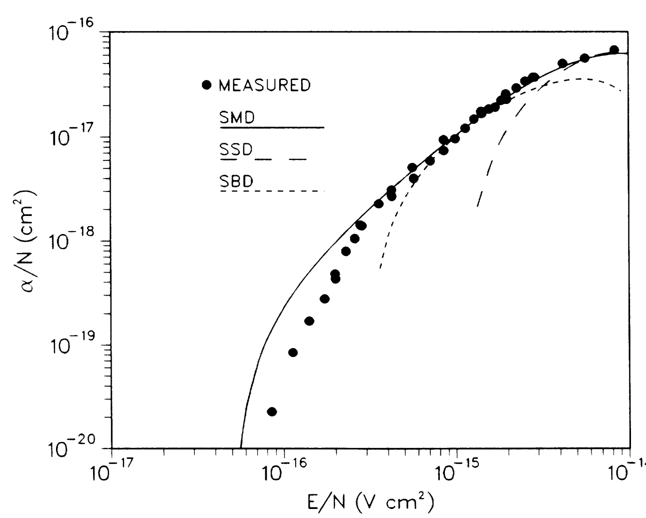

FIG. 2. Comparison of calculated values of α/N with measured values: SMD-shifted Maxwellian; SSD-shifted shell; SBD-single beam (energy).

shown as curve SBD (ENERGY) in Fig. 3, and that from Eq. (37) and (39) as curve SBD (MOMENTUM). The SBD (ENERGY) result in Fig. 3 is identical to that obtained by Sommer *et al.*[7] Clearly, the single beam model based on the energy balance equation is more accurate than that based on the momentum balance equation, as found by others.[15]

Corresponding values of random energy U_r and directed energy U_d are shown in Fig. 4 for SMD, and in Fig. 5 for SSD. Note that the ratio of directed energy to random energy is on the order of 10^{-4} for values of E/N near 10^{-17} V cm^2 where elastic collisions dominate energy balance, but increases to a value on the order of unity near $E/N = 10^{-14}$ V cm^2 where inelastic collisions dominate energy balance. Note also from Fig. 5 that U_r levels off near the excitation energy $eV_x = 21$ eV for SSD, where it stays until E/N gets very large. This behavior is consistent with the large error in α/N for values of E/N below about $5x\,10^{-15}$ shown in Fig. 2 for SSD.

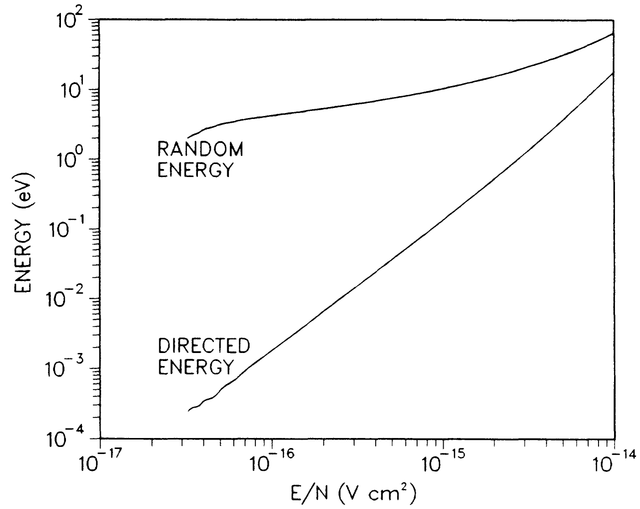

FIG. 4. Random energy U_r and directed energy U_d vs E/N for shifted Maxwellian distribution.

B. Comparison with Monte Carlo–Boltzmann (MC-B) calculation

Monte Carlo simulation of electron kinetics in a steady, uniform electric field with finite electrode separation has been published, along with companion Boltzmann calculations.[16] The main result of these two calculations is a definition of nonequilibrium regions near the electrodes. In this section comparisons are made between these MC-B calculations and five-moment calculations for shifted Maxwellian and shifted shell distributions.

Near the electrodes, the assumption that the electrons are in equilibrium with the field is invalid because directed energy and random energy both change with position. Therefore, Eqs. (35) and (36) must be solved numerically for $U_d(z)$ and $U_r(z)$. In the present work, this is done by a Runge-Kutta technique. As in the MC-B calculations,[16] the electric field is taken to be independent of distance from the cathode surface.

Two boundary conditions are required to get unique solutions to Eqs. (35) and (36). Specification of $U_d(0)$ and $U_r(0)$ at the cathode surface seems reasonable, but what are the proper values to assign to these quantities? It is known that electrons ejected from metallic surfaces by impinging ions come off in all directions and have energy of a few eV. Consequently, it is reasonable to assume that the EEDF is a monoenergetic *swarm*, i.e., the EEDF is isotropic in the *forward*, $+z$ direction, with initial total average energy of $eU(0) = 5$ eV. In mathematical form, this distribution is

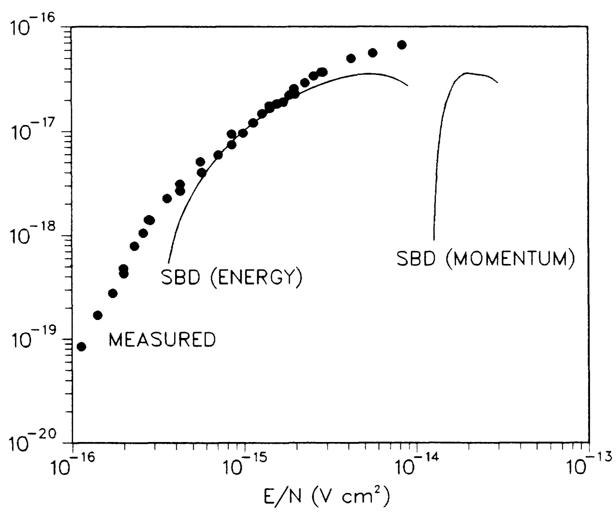

FIG. 3. Comparison of calculated values of α/N with measured values: SBD (energy)-assuming energy balance; SBD (momentum)-assuming momentum balance.

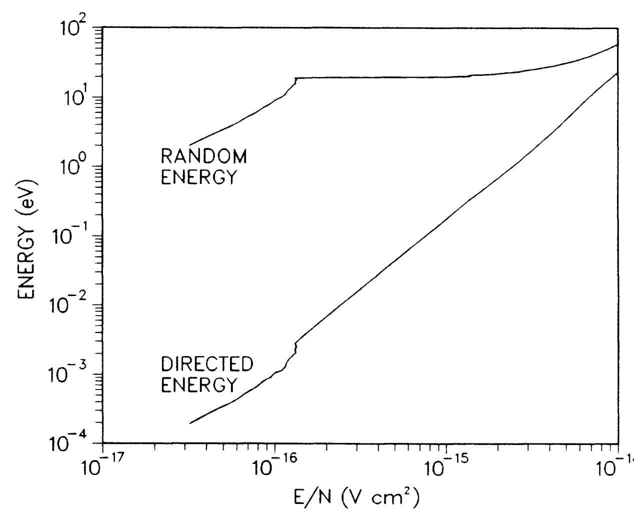

FIG. 5. Random energy U_r and directed energy U_d vs E/N for shifted shell distribution.

$$f(\mathbf{c})=\frac{n}{2\pi s^3}\delta(c-s),\quad 0\leq\mu\leq 1$$

$$f(\mathbf{c})=0,\quad -1\leq\mu\leq 0 \tag{40}$$

where the random speed s is determined by the relation $U(0)=U_r(0)+U_d(0)$. By definition, $eU_d(0)=\frac{1}{2}mw_0^2$, where $w_0=2\pi\int wfd^3c$; likewise, $eU_r(0)=\frac{1}{2}ms^2$. According to Eq. (40), the average velocity w_0 is

$$w_0=\langle w\rangle\equiv\frac{2\pi}{n}\int wf\,d^3c$$

$$=s\int_0^\infty\int_0^1\bar{c}\mu\delta(\bar{c}-1)\bar{c}^2d\bar{c}\,d\mu=\frac{s}{2}\;. \tag{41}$$

Therefore, $eU_d(0)=\frac{1}{8}ms^2$, and $eU(0)=5\text{ eV}=\frac{5}{8}ms^2$, so that $eU_d(0)=1$ eV and $eU_r(0)=4$ eV. However, Runge-Kutta integration of Eqs. (35) and (36) with these starting values results in no physically meaningful solutions for $U_r(z)$ and $U_d(z)$ extending over the required distance between electrodes. Consequently, another scheme was developed to get physical solutions.

A method which results in physically meaningful solutions consists in starting the integration very near equilibrium and integrating in both $+z$ and $-z$ directions until solutions extending the required distance between electrodes are obtained. Specifically, $U_d(0)$ is chosen to have exactly the equilibrium value and $U_r(0)$ to have slightly less than the equilibrium value, determined from Eqs. (37) and (38) at the starting point. Solutions obtained in this way for $E/N=282$ Td are compared with MC-B calculation in Figs. 6–8.

Figure 6 shows the comparison of Townsend's first ionization coefficient $\alpha(z)$, along with a straight line representing the measured value.[14] While the MC-B solutions are close together, both peak at values somewhat lower than the value obtained by measurement.

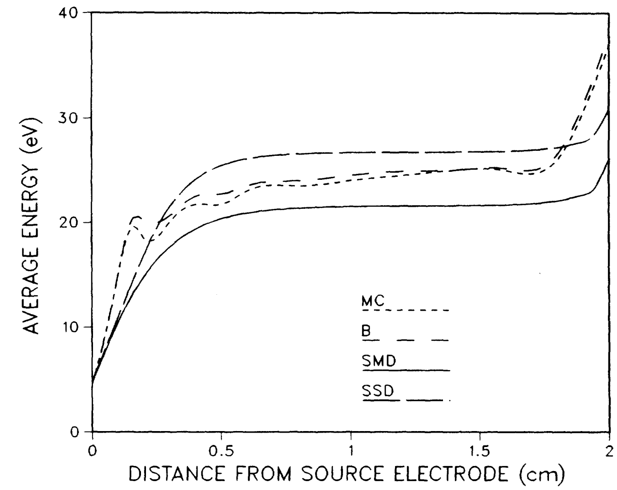

FIG. 7. Comparison of calculated average energy vs distance for $E/N=282$ Td, gas density of 3.53×10^{16} cm^{-3}, and electrode spacing of 2 cm. Monte Carlo–Boltzmann results from Ref. 16.

The curve for SMD peaks at a value which is closer to the measured value, in agreement with the equilibrium result shown in Fig. 2. The curve for SSD peaks at a value considerably lower than those of the other curves, also in agreement with the corresponding equilibrium result shown in Fig. 2. It is interesting to note that the SSD result for $\alpha(z)$ shows a region of about 0.25 cm in length near the cathode where there is no ionization, as do the MC-B results. This region of no ionization is where the EEDF is being accelerated to ionization threshold. Note that the MC-B curves rise much more sharply than does the SSD curve, and quickly approach the SMD curve.

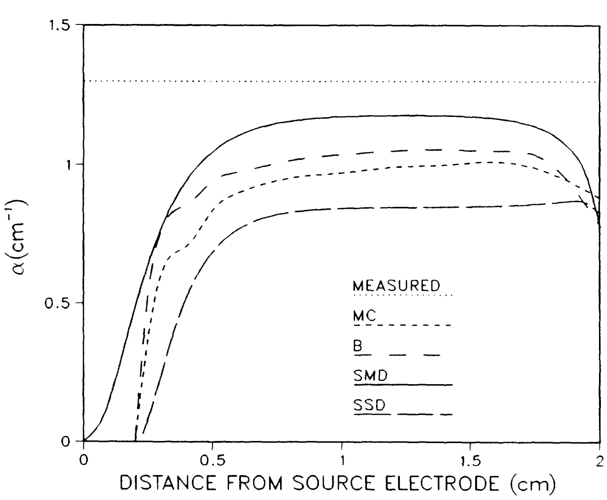

FIG. 6. Comparison of calculated Townsend α vs distance for $E/N=282$ townsend (Td), gas density of 3.53×10^{16} cm^{-3}, and electrode spacing of 2 cm. Monte Carlo and Boltzmann results from Ref. 16.

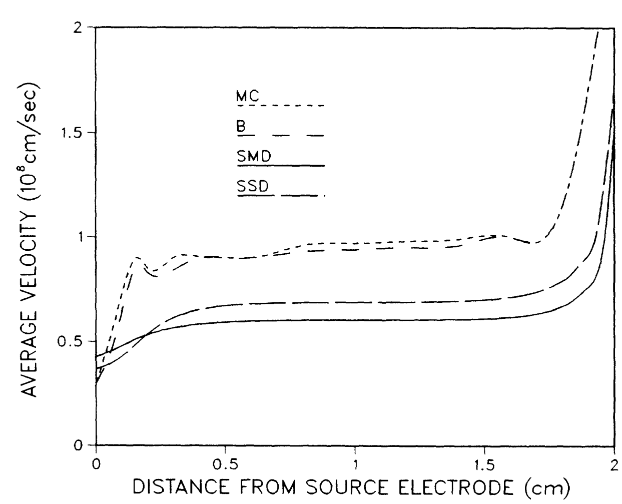

FIG. 8. Comparison of calculated average velocity vs distance for $E/N=282$ Td, gas density of 3.53×10^{16} cm^{-3}, and electrode spacing of 2 cm. Monte Carlo and Boltzmann results from Ref. 16.

The SMD curve can be made artificially to coincide approximately with the MC-B curve in this region by assuming that there are no electrons with energy greater than eEz at each point z when calculating $\alpha(z)$. The advantage of doing so, however, is not clear. The reason why the MC-B curves do not peak at a value closer to the measured value is not known. Perhaps slightly different values for the cross sections were used in the calculations.

Figure 7 shows the comparison of average energy versus position. Note that the MC-B result rises more sharply near the cathode than does the moment result. The initial slope of the MC-B curve is given by the equation

$$\frac{dU}{dz}=E , \tag{42}$$

where U is the average (total) energy of the electrons. By Eq. (36), the initial slope of the SMD (or SSD) curve is given by the relation

$$\frac{dU}{dz}\approx\frac{dU_r}{dz}\approx\tfrac{3}{5}E , \tag{43}$$

for large values of E, when random energy U_r at the cathode is much greater than directed energy U_d, and by the relation

$$\frac{dU}{dz}\approx\frac{dU_d}{dz}\approx E , \tag{44}$$

when the opposite is true. The initial slope of the SMD cure in Fig. 7 is given approximately by Eq. (43) because $U_d(0)\approx 0.5$ V and $U_r(0)\approx 4.5$ V.

The MC-B curves in Figs. 7 and 8 give $U_r(0)\approx 4.25$ V and $U_d(0)\approx 0.25$ V, i.e., $U_d(0)\ll U_r(0)$. However, the initial slope is obviously given by Eq. (42), not by Eq. (43). A basic assumption in the derivation of Eqs. (35) and (36) is that off-diagonal elements of the pressure tensor are negligible, and all diagonal elements have the same value—namely, $\frac{2}{3}neU_r$. Therefore, a possible explanation for the difference in initial slope between MC-B and SMD-SSD curves in Fig. 7 is that the assumption of an isotropic partial pressure for the electrons in the near cathode region is a weak assumption.

Comparison of average velocity versus position is shown in Fig. 8. The reason for the considerable difference in equilibrium value of average velocity between MC-B calculation and SMD-SSD calculation is not known. There are no measurements of average velocity at high E/N with which to compare these calculations.

C. Effect of ionization on average velocity and energy

It has been pointed out that ionizing collisions tend to reduce average energy below the value that would obtain if there were no such inelastic collisions.[6] This result is intuitively obvious from the energy balance equation, which describes in mathematical form the process by which the electron gas gives up the ionization potential energy eV_i each time there is an ionization event. But what is the effect of ionizing collisions on the average velocity? The answer lies in Eq. (37), which can be solved for average velocity w_0 to give

$$w_0=\left[\frac{2eU_d}{m}\right]^{1/2} =\frac{W}{2(1+\nu_i/\nu_m)}\left\{1+\left[1-4\frac{\nu_i}{\nu_m}\left[1+\frac{\nu_i}{\nu_m}\right]\frac{kT}{mW^2}\right]^{1/2}\right\} , \tag{45}$$

where U_r has been replaced by $\frac{3}{2}kT$ and drift velocity W has been written for the quantity $eE/m\nu_m$. According to this equation, w_0 is less than W for two reasons. First, the acceleration of newly created electrons to the average velocity must be taken into account. The effect of this process of acceleration is described mathematically by the term $1+\nu_i/\nu_m$ in the denominator of Eq. (45). Second, when ionization takes place, electron density increases in the direction of the electric field, causing a diffusion current of electrons to oppose the mobility current. The effect of this process of back diffusion is described mathematically by the negative term within large square brackets in Eq. (45). When $\nu_i=0$, then Eq. (45) gives $w_0=W$. Equation (45) predicts that w_0 is less than W even in cases where $\nu_i\ll\nu_m$, provided that $kT\gg mW^2$, a provision which generally obtains. Even in the special case of energy-independent momentum transfer collision frequency, therefore, the average velocity w_0 is significantly less than the drift velocity W for high values of E/N, because electron density increases with increasing distance away from the cathode, causing back diffusion to reduce average velocity.

A different conclusion was reached in the paper by Robson and Ness,[6] possibly because the importance of the density gradient term in the electron momentum balance equation was overlooked. In their paper it is argued that average velocity is equal to quantity $eE/m\nu_m$ when $\nu_i\ll\nu_m$, and that drift velocity deviates from average velocity only in that range of E/n for which the ionization rate ν_i varies with E/N. This point can be clarified by considering the following model cross section (case III A of Ref. 6):

$$Q_m(\epsilon)=\frac{10^{-15}}{\epsilon^{1/2}}\ \text{cm}^2,\quad Q_i(\epsilon)=\frac{Q_m(\epsilon)}{500}\ \text{cm}^2 ,$$

where the expression assumed for the ionization cross section Q_i applies only when ϵ is greater than eV_i; for ϵ less than V_i, $Q_i=0$. Solutions for average velocity w_0 and average energy U_r+U_d obtained from Eqs. (37) and (38) are shown plotted as solid curves in Fig. 9 for the model cross sections given above, using the following additional parameters: $V_i=10$ V and $m/M=10^{-3}$. The dashed lines in Fig. 9 represent values average velocity and average energy would have if $Q_i=0$ for all energies. The dashed curve labeled W, defined as $eE/m\nu_m$, corresponds to the curve for *average* velocity in Fig. 1 of Ref. 6. The quantity ξ is defined as $(M/m)mW^2/2e$. Note that the difference between w_0 and W in Fig. 9 increases with increasing E/N.

According to the present theory, the effect of ionizing collisions on drift velocity W and average velocity w_0, *in*

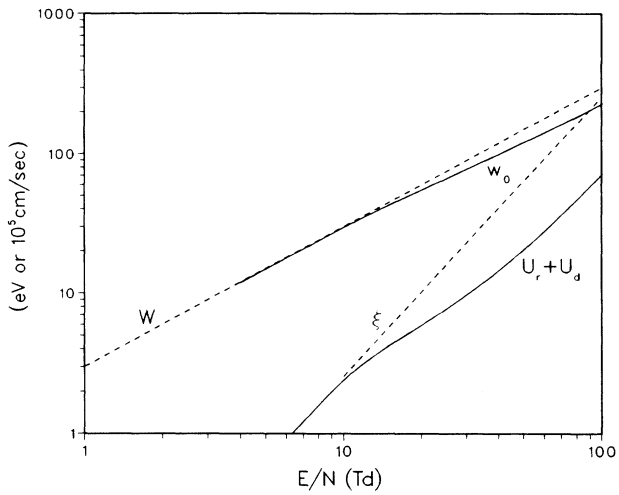

FIG. 9. Calculated average energy and average velocity vs E/N for a model gas with constant momentum transfer collision frequency, showing effect of ionization, for shifted Maxwellian distribution. Dashed lines represent values without ionization, i.e., $Q_i=0$.

the steady state, can be summarized as follows. When $\nu_m(\epsilon)$ is independent of energy, then W, defined as $eE/m\nu_m$, is unaffected by ionizing collisions, provided that $\nu_i \ll \nu_m$. However, when the momentum transfer collision frequency $\nu_m(\epsilon)$ depends on energy ϵ, then drift velocity W is affected by ionizing collisions through their cooling effect on the electron gas. Average velocity w_0 is always less than drift velocity W when ionizing collisions take place under equilibrium conditions in the steady state, because of back diffusion of electrons. Because α is inversely proportional to w_0, according to Eq. (39), it is important to have the correct value of w_0 when calculating α based on the moment method.

VI. SUMMARY AND CONCLUSION

Velocity moments of the Boltzmann equation, including moments of the collision integral for elastic and inelastic collisions, have been derived for two model distribution functions—shifted Maxwellian and shifted shell. Based on comparison of calculated results for α/N versus E/N with measurement in a steady, uniform electric field of infinite extent in helium, and on comparison of calculated results for effective ionization coeffiient $\alpha(z)$ and average energy $U_r(z)+U_d(z)$ with Monte Carlo simulations in a steady, uniform electric field of finite extent in helium, it is concluded that five-moment theory based on a shifted Maxwellian distribution is superior to either the five-moment theory based on a shifted shell distribution, or the two-moment theory based on a monenergetic beam distribution.

ACKNOWLEDGMENTS

The author is indebted to Professor H. J. Oskam of the University of Minnesota, and to Dr. A. V. Phelps of JILA, for valuable and constructive criticism of the content and format of this paper.

[1]T. J. Moratz, L. C. Pitchford, and J. N. Bardsley, J. Appl. Phys. **61**, 2146 (1987).
[2]J. Polman, Physica **54**, 305 (1971).
[3]W. H. Long, Air Force Aero Propulsion Laboratory Report No. AFAPL-tr-79-2038, 1979 (unpublished); Bull. Am. Phys. Soc. **24**, 132 (1979).
[4]P. Bayle, J. Vacquie, and M. Bayle, Phys. Rev. A **34**, 360 (1988); **34**, 372 (1988).
[5]J. Polman, J. E. van der Werf, and P. C. Drop, J. Phys. D **5**, 266 (1972); J. Polman and P. C. Drop, J. Appl. Phys. **43**, 1577 (1972).
[6]R. E. Robson and K. F. Ness, J. Chem. Phys. **89**, 4815 (1988).
[7]T. J. Sommerer, J. E. Lawler, and W. N. G. Hitchon, J. Appl. Phys. **64**, 1775 (1988).
[8]W. P. Allis, in *Motions of Ions and Electrons,* Vol XXI of *Handbuch der Physik,* edited by S. Flugge (Springer-Verlag, Berlin, 1956); Sec. 37; other moments of the collision integral are given in succeeding sections.
[9]T. F. Morse, Phys. Fluids **6**, 1420 (1963).
[10]J. H. Ingold, in Gaseous Electronics, edited by M. N. Hirsh and H. J. Oskam (Academic, New York, 1978), Vol. I, p. 36.
[11]R. W. Labahn and J. Callaway, Phys. Rev. A **2**, 188 (1969).
[12]G. D. Alkhazov, Zh. Tekh. Fiz. **40**, 97 (1970) [Sov. Phys.—Tech. Phys. **15**, 66 (1970)].
[13]J. W. McConkey, F. G. Donaldson, and M. A. Hender, Phys. Rev. Lett. **26**, 1413 (1971).
[14]J. Dutton, J. Phys. Chem. Ref. Data **4**, 722 (1984).
[15]A. V. Phelps, B. M. Jelenkovic, and L. C. Pitchford, Phys. Rev. A **36**, 5327 (1987).
[16]P. Segur, M. Yousfi, J. P. Boeuf, E. Marode, A. J. Davies, and J. G. Evans, in *Electrical Breakdown and Discharges in Gases,* Vol. 89A of *NATO Advanced Study Institute Series B: Physics,* edited by E. E. Kunhardt and L. H. Luessen (Plenum, New York, 1983), p. 331.